

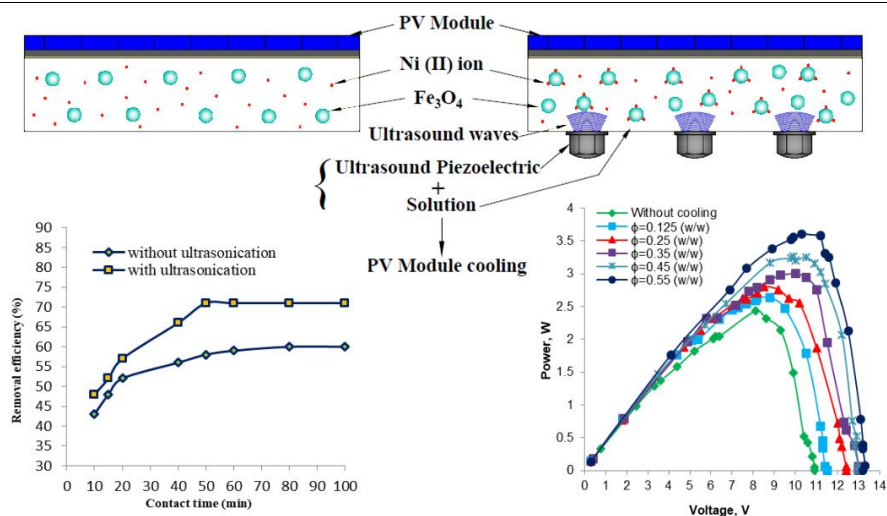


Original paper

Integrating the process of Ni (II) ions removal from aqueous solution and cooling of a photovoltaic module by 1.7 MHz ultrasound waves

Zakie Rostami¹, Masoud Rahimi^{2,*}, Neda Azimi¹¹Department of Chemical Engineering, Kermanshah Branch, Islamic Azad University, Kermanshah, Iran.²Department of Chemical Engineering, Faculty of Petroleum and Chemical Engineering, Razi University, Kermanshah, Iran.

GRAPHICAL ABSTRACT



ARTICLE INFO

Article history:

Received 30 February 2020

Reviewed 10 May 2020

Received in revised form 9 June 2020

Accepted 13 June 2020

Keywords:

Adsorption
Ultrasound
Fe₃O₄
Bentonite
Nanoparticles
Sono-separator

ABSTRACT

In this study, Ni²⁺ removal from aqueous solution was investigated by concurrent usage of Fe₃O₄ nanoparticles and a high frequency ultrasound (1.7 MHz). In addition to Ni²⁺ removal, presence of the high frequency ultrasound led to being cooled photovoltaic (PV) module. Studied variables were pH and adsorbent dose (AD). Results indicated that the Ni²⁺ removal efficiency increased with an increase in the pH ranging from 2 to 9. Furthermore, the Ni²⁺ removal efficiency boosted by an increase in the AD. However, no significant enhancement in Ni²⁺ removal efficiency was observed at the AD above 9 g. Generally, the maximum Ni²⁺ removal efficiency was about 79 % for contact time of 50 min at pH=9 and AD=9 g in the presence of ultrasound. At the efficient condition (pH=9, AD=9 g and contact time=50 min), using ultrasound showed 16-20 % enhancement in Ni²⁺ removal efficiency compared to no ultrasound usage. From heat transfer view, it was observed that propagation of 1.7 MHz ultrasound into nanofluid significantly has cooled the photovoltaic (PV) module. Moreover, an increase in concentration of nanofluid (AD) showed a positive effect on reduction of heat from the PV module surface and maximum generated power. Obtained data demonstrated that agitating nanofluid by 1.7 MHz ultrasound decreased temperature of the PV module up to 15.5 % compared to no cooling system.

©2020 Razi University-All rights reserved.

1. Introduction

The presence of pollution in water and wastewater resources is investigated as an important problem due to toxicity, non-

biodegradability, and vigorous damages in human health. Discharge of sewage, urban, industrial, and agricultural drainage has a major impact on these pollutions. An increase in the contamination of surface and ground waters by heavy metals and other pollutants from industrial

*Corresponding author Email: masoudrahimi@yahoo.com; m.rahimi@razi.ac.ir

effluents makes it necessary to find the environmental solutions in the removal of these materials. Heavy metals (Cu, Zn, Hg, Cd, Cr, Co, Ni, As, Al ...) are among the very hazardous pollutants arriving into the environment via industrial activities (Fu et al. 2011; Liao et al. 2016, Malamis et al. 2013; Wang et al. 2012). Ni (II) ions are extremely soluble, mobile, and toxic. Increasing the presence of Ni (II) ions in several industrial usages such as battery production, electroplating, smelting, mineral processing, etc., results in a high discharge of Ni (II) ions in wastewater, which is damaging for human health and the environment (Belova et al. 2016; Es-sahbany et al. 2019). For this purpose, accurate instructions have been considered for the discharge of Ni (II) into surface waters. Adsorption is efficient in the separation process in some of the natural, physical, biological, and chemical industries. This is because of the high capability of solid materials to absorb the molecules of gases or solutions. Recently, the adsorption process has been applied as one of the efficient methods for the removal of heavy metal ions, which is before other techniques because it is easy to use and has low costs (Jamshidi et al. 2016). However, the adsorption process has problems such as a little mass transfer rate, the difficulty in the regeneration with the adsorbent and limitations for development and application (Ji et al. 2006). To prevail in these problems, several modifications to the conventional adsorption process have been extensively considered. Ultrasound is a new method that can amplify the chemical and mass transfer processes and refract the bonded between the adsorbate and the adsorbent (Ji et al. 2006; Hamdaoui et al. 2009).

These impacts are due to the phenomena of shock waves, acoustic cavitation, and micro streaming. The shock wave causes the generation of the microscopic agitation within interfacial films around the solid particles. Acoustic cavitation is the formation, growth, and the collapse of micrometer-scale bubbles produced by the propagation of ultrasound waves into a liquid medium. Acoustic-micro streaming is the basis of motion in the liquid after ultrasound irradiation (Asfaram et al. 2015; Parvizian et al. 2012; Rahimi et al. 2015). These phenomena originated from the propagation of ultrasound energy into the adsorption process, results in the augmentation in the mass transfer rate close to the surface of the adsorbent. In addition, simultaneous using the nanoparticles as the absorbent of the metal ions and the irradiation of ultrasound into the aqueous solution could break up the aggregates of nanoparticles. Furthermore, ultrasound acts like an agitator or a mixer and could apply the powerful mechanical forces in the solution, so; it could reinforce the mass transfer rate in the solid-liquid interface (Mondragon et al. 2012; Zou et al. 2014). Using the ultrasound with the frequency spectrum above than 1 MHz in mass transfer processes is confined in the literature.

In this research, a reservoir is attached to the behind of a PV module and six piezoelectrics that produce the ultrasound waves are located on it, intensifying Ni (II) removal process, and cooling the PV module. Cooling of the PV modules is an important issue because according to the literature (Ghadiri et al. 2015; Sardarabadi et al. 2014), during the operation of the PV module only about 15 % of the incident solar energy is changed to electricity and the remaining energy is converted to heat raises the temperature of the modules. The absorbed heat leads to increasing the temperature of the PV system, which leads to reducing its electrical conversion efficiency by 0.45 % for a 1 °C rise of the working temperature (Ghadiri et al. 2015; Kalogirou et al. 2006; Sardarabadi et al. 2014). Chow et al. (2003) reported that increasing about 10 °C in the temperature of the PV module surface causes a reduction of 5 % in its electrical efficiency. Decreasing the operating temperature of the PV module is an effective method for increasing its efficiency and the power output without damaging the PV unit. This problem can be resolved by cooling and heat dissipation from the PV surface during its operation. A review of the literature depicted that one alternative to forbear the temperature increment of the PV modules is using nanofluids as working fluid (An et al. 2016; Hussien et al. 2015; Khanjari et al. 2016; Radwan et al. 2016). Researches on this subject have transpired owing to the possible mechanisms that lead to such effective heat transfer improvement. Fluids have a lower thermal conductivity compared to metal suspensions. Therefore, adding the small amounts of metallic and other nanoparticles in the carrier fluid (known as nanofluids) lead to a large increase in their thermal conductivity and so heat transfer rate (Ghadiri et al. 2015).

Karami et al. (2014) used the water-based nanofluid comprising Boehmite nanoparticles to improve the cooling performance of a PV module. Results depicted that the application of nanofluid as a working fluid result in a higher reduction in the average surface temperature of the PV module and has a positive effect on cooling performance. Later, Karami et al. (2014), evaluated the cooling performance of water-based

Boehmite nanofluid in a hybrid photovoltaic (PV) module. Their results depicted a 27 % improvement in the electrical efficiency for 0.01 wt. % concentration of the nanofluid. Hussien et al. (2015) depicted the enhancement of the electrical efficiency and the thermal performance of a Hybrid Photovoltaic/Thermal system (PV/T) by applying nanofluids as the working fluid. Sardarabadi et al. (2016) and Al-Waeli et al. (2017) to improve electrical and thermal efficiencies of PV/T systems by nanofluids have accomplished similar studies. In these studies, the higher electrical efficiency of nanofluid had been reported rather than pure water. Suresh et al. (2018) used various nanofluids to reduce the temperature of the PV panel by increasing the thermal conductivity of base fluids.

According to our survey, there are no available research studies on the simultaneous application of using ferrofluid and ultrasound energy to cool the PV module and removing the metal ions from aqueous solution. Simultaneous using the nanofluid and high frequency ultrasound is perused as an active cooling method for a PV module and besides this idea can be used to intensify the adsorption process of heavy metals. The major difference of this study with the above-mentioned researches (Belova et al. 2016; Es-sahbany et al. 2019; Menkah et al. 2019) is that the experiments had been undertaken in the present work are the adsorption of Ni (II) ions onto Fe₃O₄ nanoparticles while the process amplified by 1.7 MHz ultrasound waves. Ultrasonic waves with the frequency in the range of MHz are capable to induce the strong acoustic streaming which is responsible for the augmentation of the rate of adsorption processes. In this study, Ni (II) ions removal process from the aqueous solution is integrated with the cooling of a photovoltaic (PV) module. Indeed, the cooling of the photovoltaic module is done by contacting the nanofluid, including Fe₃O₄ nanoparticles, which are located in the reservoir connected to the back of the PV module. The base fluid is water that contains Ni (II) ions, which is changed to ferrofluid by adding Fe₃O₄ nanoparticles. The presence of Fe₃O₄ nanoparticles in the aqueous solution (0.125-0.55 (w/w)) act as the Ni (II) absorbent and multiplier the thermal conductivity of the base fluid to cool the PV module. The measured results for the influence of pH, adsorbent dose, and contact time on Ni (II) ions removal, the surface temperature of the PV module and maximum power generated by the PV module have been reported.

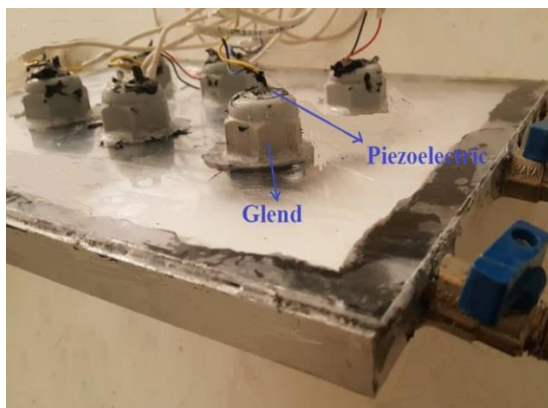
2. Experimental works

2.1. Experimental setup and apparatus

Real photograph of the experimental setup discussed in this research, the pictures of the back of the photovoltaic module, and glend arrangements are depicted in Fig. 1. The fundamental parts of the constructed system are; a PV module, a solar modeler, ultrasound transducers, an reservoir, and a data attainment system. An aluminum framework is utilized to take the PV module below the light of halide lamps in a fixed situation. In order to evaluate the temperature of the PV module at several points on it, twelve thermocouples are put on the upper surface of the PV module. A very thin layer of thermal epoxy glue rubbed on the tip of each thermocouple. Six piezoelectrics engaged to create the ultrasonic with a frequency of 1.7 MHz. This apparatus applied to mix the aqueous solution containing Ni (II) ions available in the reservoir attached to the back of the PV module. The reservoir built of strong plastic has the benefit to control the fluid temperature at a constant value within the experiments. Fig. 2 represents a schematic illustration of the experimental setup and the thermocouple statuses.



(a)



(b)

Fig. 1. (a) Real picture of designed setup used in the present research, (b) Real picture of the backside of photovoltaic module and glend arrangements.

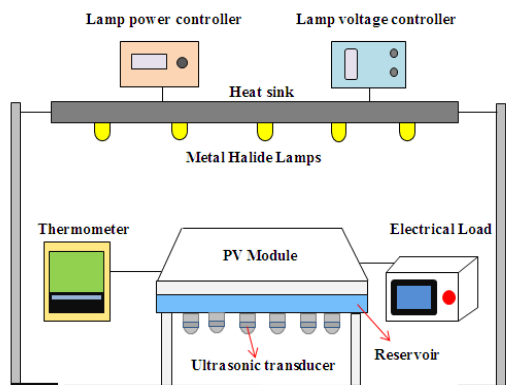
A thermometer (BTM-4208SD model) manufactured by Lutron company and a Voltage-Ampere measurement is used to measure the surface temperature and the electrical output of the PV module, respectively. A solar simulator is built and applied to emulate the necessary solar radiance for the experiments. Because the natural sunshine is not continually existed, five Metal Halide (MH) lamps are utilized to turn out a continuous spectrum of light. The effective area of one matrix in the PV module is 24 mmx36 mm. Five MH lamps are situated under the ceiling of the aluminum framework at a distance of 50 cm from the PV module. Each piezoelectric transducer inside the Glend is posited between two rubber gaskets to prevent fluid leakage. Because of the elasticity of the rubber gaskets, it cannot prohibit the vibration of the piezoelectric transducer. In order to prevent fluid leakage, surrounding the Glends on the body of the reservoir are sealed with silicone glue.

In all experiments, deionized water (DI-water) is used to make the processes more efficient. A solution of Ni (II) is prepared by dissolving Ni (NO₃)₂.6H₂O in DI-water, and that solution is diluted to the desired concentration for actual use. Firstly, 100 mg of Ni(NO₃)₂.6H₂O powder is dissolved in 1 liter of DI-water in a separate container (initial concentration of 100 mg/L). Then, the desired solution is completely mixed by using a shaker at 150 rpm at room temperature (25 °C). In order to determine the effect of pH; NaOH and HCL solutions with 0.1 molar concentrations are used and pH is measured using pH meter (model: Eutech pH 700, Singapore). In this study, the impact of adsorbent dose (Fe₃O₄ nanoparticles) on the elimination of Ni (II) ions from the base solution is investigated. The adsorbent dose is investigated as a variable with the domain of 2.5-11 g (2.5, 5, 7, 9, 10, and 11) Fe₃O₄ nanoparticles. In order to make each solution, a certain amount of adsorbent dissolved in the solution containing Ni (II) ions. At this step, each solution containing Ni (II) ions and adsorbent at four different pH values of 2, 4, 7 and 9 are investigated. The nanoparticles of Fe₃O₄ manufacturing of Asia-Pacific Co. has been used as the adsorbent. Magnetic nanofluid of Fe₃O₄ nanoparticles is prepared by adding the desired amount of Fe₃O₄ nanoparticles into a 2L aqueous solution at room temperature.

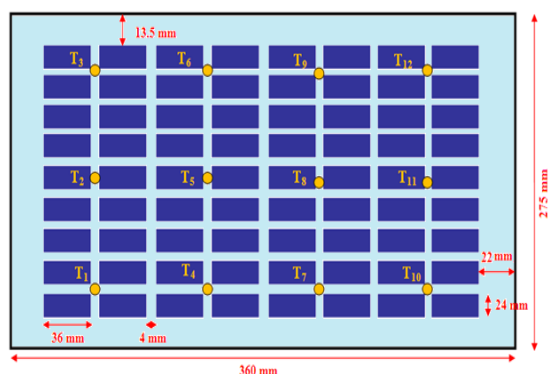
2.3. Experiment steps

Before the testing, the leak-trial with deionized water is attentively fulfilled. After resolving all leaks, ultrasound transducers and MH lamps are turned on. The amounts of the output voltage at several electrical currents are set using the electrical load system (ELS). During the testing, the electrical output of the PV module is connected to the ELS. When the system comes close to the steady-state (after 50-60 min) condition, I-V values are registered to specify the maximum power point (Pmax), the values of current I (Imax in A) and voltage V (Vmax in V) at the maximum power of the PV module. The temperatures of 12 points on the upper and bottom surfaces of the PV module are seized by the data attainment system. The average amount of these 12 temperatures is recorded for calculation of the temperature of the PV module. All the trials are accomplished at room temperature and the radiation severity of 1000 W/m².

Besides, the Fe₃O₄ nanoparticles are well dispersed in the solution containing Ni (II) ions as the base liquid. Because of the significant differences between the density of Fe₃O₄ nanoparticles and the base fluid, the settlement of the Fe₃O₄ nanoparticles at the bottom of the beaker is expected. Therefore, for each experiment, nanoparticles of the required quantity are slowly added to the suspension contains Ni (II) ions and the obtained mixture after simple mixing are poured into the reservoir attached to the back of the PV module, the piezoelectric actuators switched on the ultrasonic transducers, and then ultrasonic waves propagate into the solution. In the presence of high-frequency ultrasonic waves (1.7 MHz), the need for mixing with a mechanical stirrer is eliminated because the ultrasonic waves with frequency in the range of MHz are able to generate more intense convective flows and acoustic streaming which it can prevent the nanoparticles settlement. On the other words, 1.7 MHz ultrasonic waves are capable to generate vigorous micro-streams besides the cavitation effects, which can keep nanoparticles in a floating condition (Parvizian et al. 2012; Rahimi et al. 2013). The nanoparticles can still keep dispersing well after the sonicated nanofluid in the operation condition has been standing for 12 hours and no sedimentation is observed. The solution in the reservoir is subjected to ultrasound waves for a specified period. After the prescribed time, the solution is removed from the reservoir and finally, the solution is analyzed to determine the recovery rate of Ni (II) adsorption. All experiments are fulfilled at room temperature and each assay is repeated three times, and the average of the three obtained values is reported as the final amount of adsorbed Ni (II) ions.



(a)



(b)

Fig. 2. (a) Schematic plan of the designed setup used in this study, (b) The scheme of the upper surface of the PV module and the location of the thermocouples.

2.2. Materials and solution preparation

2.2.1. Preparation of aqueous solution and Fe₃O₄ nanofluid

2.4. Experimental data processing

When the time of the adsorption is long enough, the adsorption system reaches to equilibrium state and thus the equilibrium amount adsorbed of Ni(II) ions can be calculated by Eq. 1 (Mousavi et al. 2019; Nayeri et al. 2019).

$$q_e = \frac{C_0 - C_e}{m} V \tag{1}$$

where, q_e is the absorption capacity of Ni(II) ions in equilibrium state, C₀ and C_e are the initial and final concentration of Ni (II) ions in solution, respectively. V is the volume of solution, and m is the mass of

adsorbent. The removal efficiency of Ni (II) ions was calculated as follow (Nayeri et al. 2019; Mousavi et al. 2019).

$$\text{Removal efficiency} = \frac{C_0 - C_e}{C_0} \times 100 \quad (2)$$

3. Results and discussion

3.1. Effect of pH on the adsorption of Ni (II) ions

pH is a key factor in the absorbing of heavy metal ions from solutions. Therefore, pH dependence is investigated for the removal of Ni (II) ions at a constant contact time in both layouts of with and without ultrasound (US) waves. Fig. 3 shows the percentage removal of Ni (II) ions from the solution at the temperature of 25 °C, adsorbent mass (m) of 2.5 g, and contact time=40 min. At this step, all PZTs on the body of the reservoir switched on and the ultrasound waves propagated into the aqueous solution. As shown in Fig. 3, for both layouts, the efficiency of Ni (II) elimination increased with pH and it has the highest amounts of Ni (II) removal at pH=9. In fact, pH is one of the most important parameters for controlling the adsorption process of metal ions. There are two main factors influencing the effect of pH on the adsorption of metal contaminants on the magnetic nanoparticles. One of them is the metallic pollutant ion, and the other is the surface of the adsorbent. In this section, the effect of pH on each of these factors investigated separately. The surface of Fe₃O₄ nanoparticles has a negative charge.

In order to have a high adsorption capacity, the pollutant must have a positive charge. Fe₃O₄ nanoparticles can easily be converted to iron hydroxide (II) and (III). In order to consider the impact of pH on the metal contaminants, it should be noted that the metals in the acidic environments are ionic and when they enter the base environment, they lose their ionic state and react with the OH⁻ groups in the environment. This process causes the metal to lose its positive charge and become neutral or negative (in the complexation between metal and OH⁻ groups). Therefore, according to the mentioned factors, there is only a small range of acid-to-base pH, in which the amount of metal ion adsorption on the surface of adsorbent is high. Optimization studies showed that the optimal pH value is about 9, which indicates that at this pH, the magnetic adsorbent and nickel-metal ions are completely active in the environment. According to Fig. 3, it can be seen that with increasing pH, the amount of Ni (II) ion adsorption increased, so that at pH=9 and pH=2, the maximum and the minimum values have been obtained, respectively. Fig. 3 shows that by using 1.7 MHz ultrasound, the removal percentage of Ni (II) ions increased. It concluded that acoustic and micro-streams induced by high-frequency ultrasound have a high ability to induce mixing and strong mechanical effect inside the reservoir. In addition, micro-jets generated by high-frequency ultrasound collided with the surface of nanoparticles and so the adsorption of Ni (II) on the adsorbent is increased.

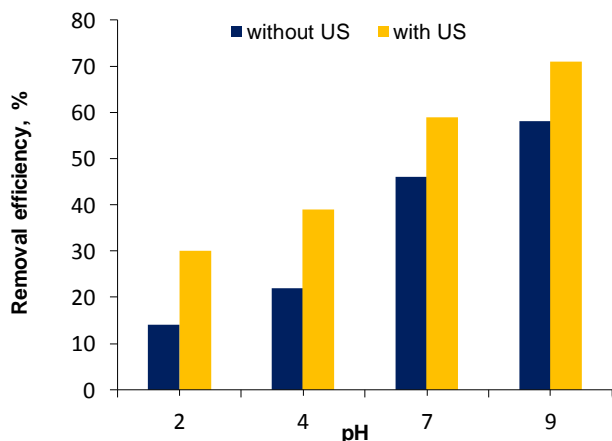


Fig. 3. Removal efficiency of Ni (II) with and without ultrasound at m=2.5 g, T=40 min.

3.2. Influence of contact time on the adsorption of Ni (II) ions

Fig. 4 shows the time-dependent removal behavior of Ni (II) ions from aqueous solution using the magnetic adsorbent. As shown, for both layouts, the amount of Ni (II) removal increases with increasing the contact time and the equilibrium time from 10 min to 50 min. However, concerning the layout without ultrasound (US), the removal rate of Ni

(II) ions from the contact time between 10 min and 80 min is still increasing and in 80 min, the percentage of removal is equal. In fact, the percentage of Ni (II) removal for without US reached its maximum value of 60 % within 80 min.

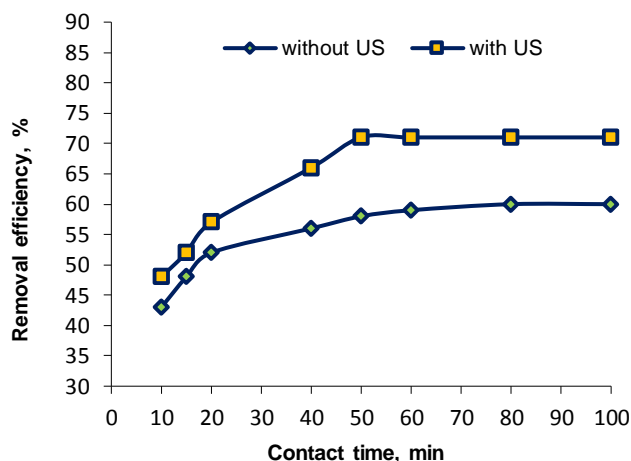


Fig. 4. Influence of contact time on the removal efficiency of Ni (II) with and without ultrasound at m=2.5 g and pH=9.

The initial adsorption rate is very fast to adsorb Ni (II) ions due to a large number of sites on the nanoparticles. According to the results obtained for the layout without ultrasound, the contact time of 80 min is chosen as the most influencing contact time to remove Ni (II) ions. However, as shown in Fig. 4, by using ultrasound, the removal rate of Ni (II) is very fast in the first 2-50 minutes, and its maximum value at a contact time of 10 min reached to 78 % and after that, the removal rate of Ni (II) ions is constant. In fact, the adsorbent surface and its sites initially increased by ultrasound propagation into the solution, and hence, the adsorption rate of Ni (II) is high. After 50 min, it may be the desorption process occurred and Ni (II) ions transferred from the surface of the adsorbent to the aqueous solution due to the discharge of Ni (II) ions from the adsorbent surface. This means that high-frequency ultrasound waves can eliminate high percentages of Ni (II) ions from aqueous solution, due to the inducing micro-streams and acoustic cavitation phenomena. Propagation of ultrasound waves into the reservoir increases the adsorption rate over a short time using a small amount of adsorbent material. Ultrasound through secondary activities such as cavitation (nucleation, growth, and temporary collapse of small gas bubbles) increases the mass transfer through the physical phenomena such as micro-streams, micro-turbulences, acoustic waves (or shock), and micro-jets. These phenomena occurred without significantly altering the equilibrium properties of the adsorption/desorption system. According to the results obtained for using ultrasound, the contact time of 50 min selected as the more efficient contact time for the elimination of Ni (II) ions under the influence of high-frequency ultrasound waves.

3.3. Influence of adsorbent dose on the adsorption of Ni (II) ions

In order to consider the influence of adsorbent dose (AD) on the Ni (II) ions adsorption, six other values for adsorbent (2.4, 5, 7, 9, 10 and 11 g of the magnetic nanoparticles) in 2 liters of Ni (II) solution are tested. Fig. 5 shows the influence of the adsorbent dose on Ni (II) ion removal from aqueous solution. Based on this figure, the adsorption rate of Ni (II) ions increased by adsorbent dose due to increasing its surface area. Increasing the specific area and the availability of more active adsorbent sites in a higher amount of adsorbent is associated with an increase in adsorption rate. By using the ultrasound, the highest removal percentage of Ni (II) is 79 % with the contact times of 50 min. In both cases, the efficient amount of adsorbent is 9 g and no significant increase is observed with increasing adsorbent dose more than 9 g (0.35 % (w/w) nanofluid) for Ni (II) removal.

3.4. Influence of initial concentration of Ni (II) ions on the adsorption process

The influence of the initial concentration of Ni (II) ions is another parameter studied. In all experiments of before sections, the initial concentration of Ni (II) is 0.1 g/L. In this section, three other concentrations (0.05 g/L, 0.15 g/L and 0.2 g/L) are investigated. Fig. 6 shows the impact of the initial concentration of Ni (II) ions in the

aqueous solution on its percentage removal at AD=9 g and pH=9 while all PZTs are activated.

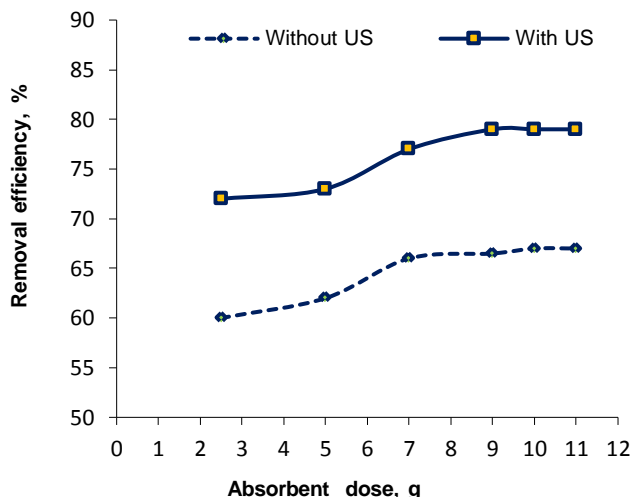


Fig. 5. Influence of adsorbent dose (g) on the removal efficiency of Ni (II) with and without ultrasound at pH=9 (Time=50 min).

From Fig. 6, it can be concluded that there is high dependence between the elimination efficiency and the initial concentration of Ni (II) ions. Therefore, by increasing the initial concentration of Ni (II) ions, the available adsorbent sites are reduced and so the removal efficiency decreased. Since in the low concentration of Ni (II) ions, available sites on the adsorbent surface are greater. As shown in Fig. 6, by an increase in the concentration of Ni (II) ions from 0.05 to 0.1 g/L, the percentage of Ni (II) ions removal increased from 77.6 % to 79 %, respectively. While by increasing Co from 0.1 to 0.15 and 0.2 g/L, the percentage of Ni (II) ions has a decreasing trend, which is due to the reduction of the adsorption capacity of Ni (II) by nanoparticles and filling their capacity. By increasing the initial concentration of Ni (II) ions in the solution, the removal efficiency is reduced. Increasing the initial concentration of Ni (II) ions causes less adsorbed sites to adsorb more Nickel in the solution. Therefore, the adsorbent in lower initial concentration has better adsorption properties.

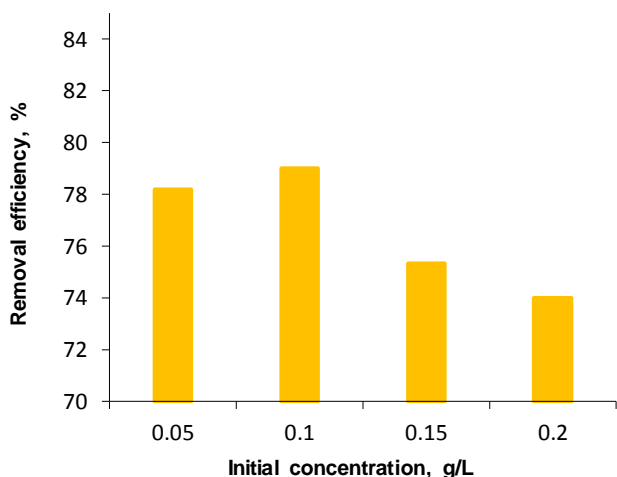


Fig. 6. Influence of initial concentration of Ni (II) on its elimination efficiency using ultrasound at AD=9 g and pH=9 (Time=50 min).

3.5. Adsorption isotherms

The adsorption of Ni (II) significantly affects by the initial concentration of Ni (II) ions in the aqueous solution. In this section, the initial concentration of Ni (II) varies from 50 to 200 mg/L, while the adsorbent dose is 9 g, pH=9, and the contact time is 50 min for use of the ultrasound. Experimental data are adapted to Langmuir and Freundlich isotherm models. Langmuir isotherm model is used to explain the chemical composition and coating of an absorber layer on the nanoparticles, and its linear form could be explained by the following equation (Sayadi et al. 2016).

$$\frac{C_e}{q_e} = \frac{1}{K_L q_m} + \frac{1}{q_m} C_e \tag{3}$$

where, q_e is the amount of Ni (II) adsorbed in equilibrium state in mg/g, C_e is equal to the concentration of Ni (II) in the solution in mg/L, q_{max} and K_L are the Langmuir constants, indicating the adsorbent saturation capacity and the energy term. By data fitting with the Langmuir model, as shown in Fig. 7 (a), $1/q_m$ is equal to 0.9040, that means $q_m = 1.105$ g/L and $K_L = 5.6568$ L/g.

The Freundlich isotherm model illustrates the distribution of active and energy sites and heterogeneous adsorbent surfaces by the following equation (Sayadi et al. 2016).

$$q_e = K_f C_e^{1/n} \tag{4}$$

where, K_f and $1/n$ are Freundlich constants related to absorption capacity and absorption intensity. As shown in Fig. 7b, in the Freundlich model, the value of n is equal to 1.196 and $K_f = 0.5161$. The comparison between these two models shows that both models are well fitted with experimental data, and of course, the value of R^2 is higher in the Langmuir model, and therefore the data compatibility with this model is greater.

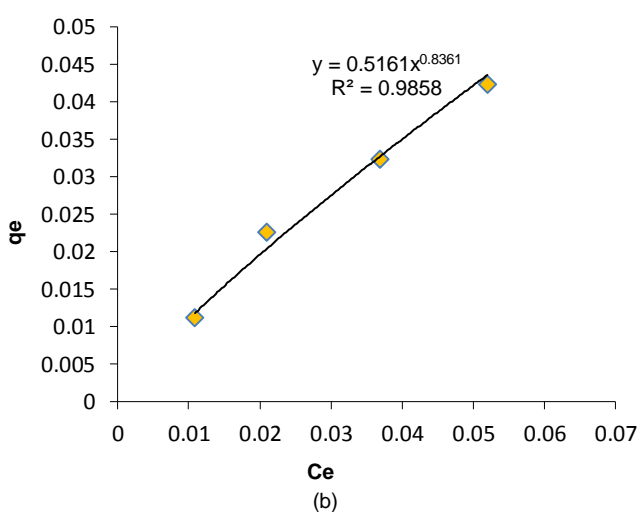
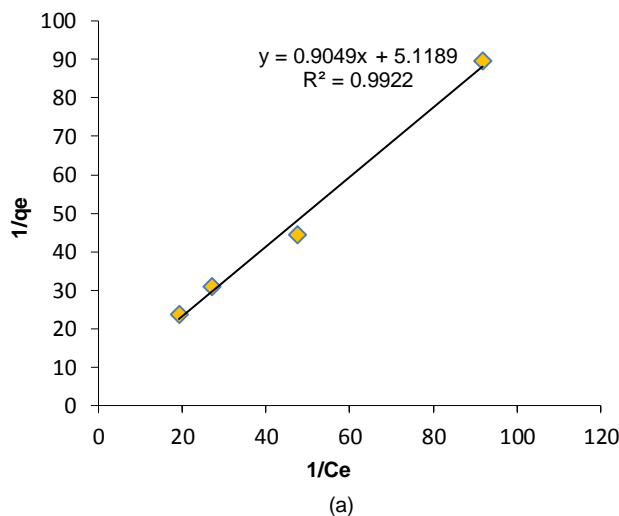


Fig. 7. Data fitting by (a) Langmuir adsorption model, (b) Freundlich adsorption model using ultrasound at AD=9 g and pH=9 (Time=50 min).

3.6. Cooling of the PV module

As it was mentioned, the temperatures of 12 points on the surface of the PV module are registered in each 5 min until the system attains to a steady-state condition (after nearly 60 min), the situation that the PV system gets maximum efficiency. Fig. 8 illustrates the alteration of T_{surf} with no cooling at the solar radiation of 1000 W/m^2 . As this figure

shows, after about 60 min, the PV system overtakes the steady-state situation and T_{surf} approaches to 52 °C.

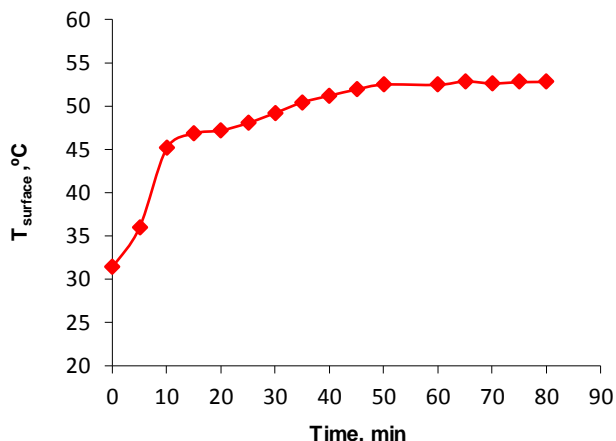


Fig. 8. Variation of the average temperature of the PV module surface without cooling.

Fig. 9 represents the changes in T_{surf} by the time for no cooling system and different weight percentages of nanofluid. The impacts of using nanofluid on T_{surf} are also seen in this Fig. By applying ultrasound, nanofluid with the concentration of 0.125 % (w/w) has the highest T_{surf} and its value at steady-condition is overtakes to 48.6 °C. 0.55 (w/w) nanofluid exhibits a lower temperature (45.1 °C at steady-condition) and more efficient cooling performance. As it is obvious in this figure, by using nanofluid, the cooling system acts in a more efficient way compared with no cooling system. It has a growing tendency with nanofluid concentration. Increasing the weight percentages of nanofluid from 0.5 % (w/w) to 0.55 % (w/w) after reach to the steady-state condition has no considerable impact on the decline of T_{surf} .

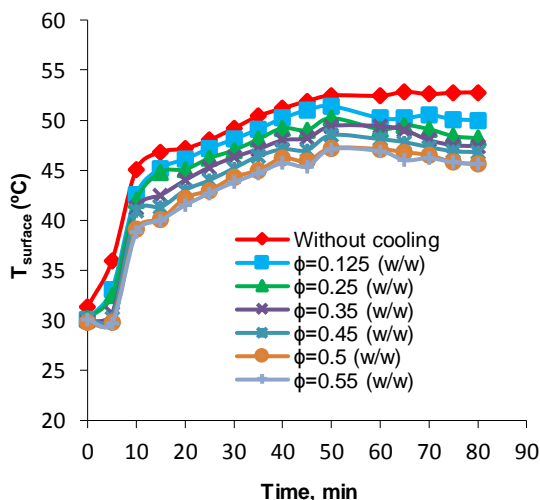


Fig. 9. Variation of the average temperature of the PV module surface by time at different concentration of Fe_3O_4 nanoparticles under ultrasound irradiation.

In order to check the impacts of ultrasound on the generated electricity by the PV module, its efficiency with no cooling system firstly is investigated. Secondly, I-V data are gathered for six different concentrations of nanofluid. As Fig. 10 shows, the area under the V-I curve develops by simultaneous application of nanofluid and ultrasound. As the region under the V-I curve displays the power generated by the PV module, these results represent progress in the output power of the PV module for using Fe_3O_4 nanofluid compared to no cooling system. The maximum generated power by the PV module (P_{max}) is computed as follows (Karami et al. 2014; Siahkamari et al. 2019).

$$P_{PV} = I_{PV} \times V_{PV} \quad (5)$$

P_{PV} by nanofluid and ultrasound is plotted versus the output voltage in Fig. 11. As anticipated, utilizing higher concentration of nanofluid shows a clear tendency in augmentation of the production capacity. The

comparison between the results of P_{PV} obtained for no cooling system and using ultrasound and nanofluid could highlight the impact of using them on the performance of the PV module. According to this figure, P_{max} belongs to the PV-ultrasound+0.55 % (w/w) nanofluid system and it is 3.65 watts, which concur with a voltage of 10.3 V.

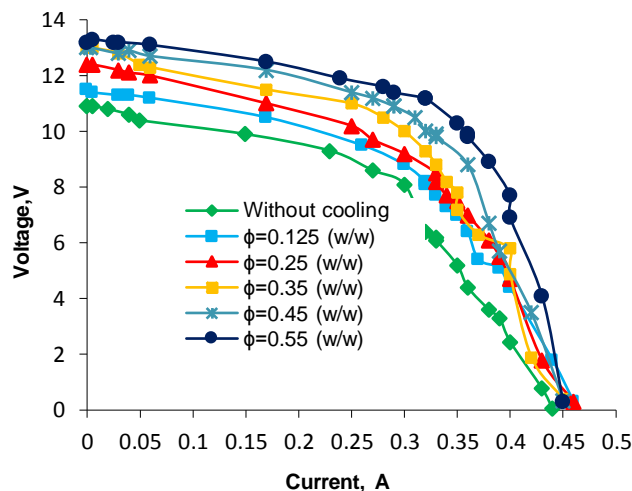


Fig. 10. Voltage-Current characteristic for different concentration of Fe_3O_4 nanoparticles at pH=9 (Time=70 min).

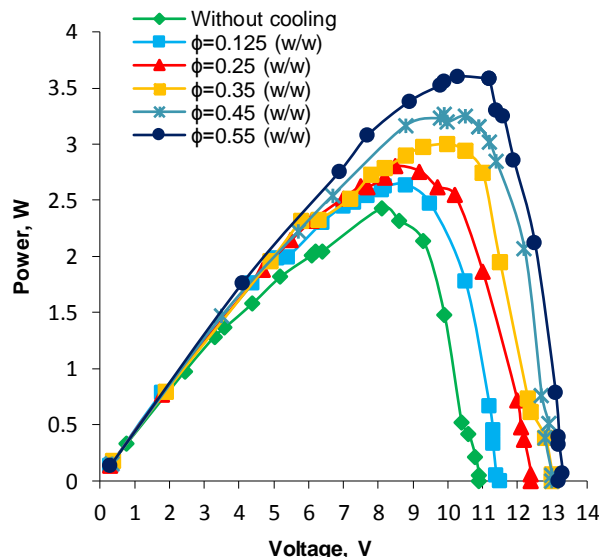


Fig. 11. Power-Voltage characteristic for different concentration of Fe_3O_4 nanoparticles at pH=9 (Time=70 min).

4. Conclusions

The effect of high-frequency ultrasound on Nickel adsorption from aqueous solution onto Fe_3O_4 nanoparticles is investigated. In this work, the processes of nickel removal from aqueous solution and the cooling of a photovoltaic (PV) module are integrated simultaneously. A reservoir is installed into the back of the PV module and the ultrasound transducers are located on it to reinforce Ni (II) removal and cooling the PV module. Indeed, Fe_3O_4 nanoparticles in the aqueous solution act as the adsorbent and augmentative of the thermal conductivity of the base fluid. The impact of pH on Ni (II) removal is studied and results showed that it increased with increase in pH from 2 to 9. The maximum Ni (II) removal rate is 79% at t=50 min and pH=9, and it approximately stayed constant after 50 min. The impact of the adsorbent dose (AD) is investigated and it is observed that Ni (II) removal increased because of an increase in the specific surface area of the adsorbent. No significant increase for Ni (II) removal is seen for ADs more than 9 g. Propagation of 1.7 MHz ultrasound into the aqueous solution and its collision on the backside of the PV module, considerably improved the cooling performance. Increasing the Fe_3O_4 nanofluid concentration (adsorbent dose) depicted positive effects on the cooling of the PV module and maximum generated power. Results depicted that the

highest reduction in the temperature of the PV module by ultrasound and 0.55 (w/w) nanofluid is about 15.5 % rather than no cooling system.

Acknowledgment

The authors would like to thank Islamic Azad University, Kermanshah Branch for providing the support to carry out this work.

References

- An W., Wu J., Zhu T., Zhu Q., Experimental investigation of a concentrating PV/T collector with Cu_3S_5 nanofluid spectral splitting filter, *Applied Energy* 184 (2016) 197–206.
- Al-Waeli A.H.A., Sopian K., Chaichan M.T., Kazem H.A., Hasan H.A., Al-Shamani A.N., An experimental investigation of SiC nanofluid as a base-fluid for a photovoltaic thermal PV/T system, *Energy Conversion and Management* 142 (2017) 547–558.
- Asfaram A., Ghaedi M., Hajati S., Goudarzi A., Bazrafshan A.A., Simultaneous ultrasonic-assisted ternary adsorption of dyes onto copper-doped zinc sulfide nanoparticles loaded on activated carbon: Optimization by response surface methodology, *Spectrochimica Acta Part A: Molecular and Biomolecular Spectroscopy* 145 (2015) 203–212.
- Belova D.A., Lakshtanov L.Z., Carneiro J.F., Stipp S.L.S., Nickel adsorption on chalk and calcite, *Journal of Contaminant Hydrology* 170 (2014) 1–9.
- Chow T.T., Hand J.W., Strachan P.A., Building-integrated PV and thermal applications in a subtropical hotel building, *Applied Thermal Engineering* 23 (2003) 2035–2049.
- Es-sahbany H., Berradi M., Nkhili S., Hsissou R., Allaoui M., Loutfi M., Bassir D., Belfaquir M., Youbi M.S., Removal of heavy metals (nickel) contained in wastewater-models by the adsorption technique on natural clay, *Materials Today: Proceedings* 13 (2019) 866–875.
- Fu F., and Wang Q., Removal of heavy metal ions from wastewaters: a review, *Journal of Environmental Management* 92 (2011) 407–418.
- Ghadiri M., Sardarabadi M., Pasandideh-fard M., Moghadam A.J., Experimental investigation of a PVT system performance using nano Ferrofluids, *Energy Conversion and Management* 103 (2015) 468–476.
- Hamdaoui O., Naffrechoux E., Adsorption kinetics of 4-chlorophenol onto granular activated carbon in the presence of high frequency ultrasonic, *Ultrasonic Sonochemistry* 16 (2009) 15–22.
- Hussien H.A., Noman A.H., Abdulmunem A.R., Indoor investigation for improving the hybrid photovoltaic/thermal system performance using nanofluid (Al_2O_3 -water), *Engineering and Technology Journal* 33 (2015) 889–901.
- Kalogirou S.A., Tripanagnostopoulos Y., Hybrid PV/T solar systems for domestic hot water and electricity production, *Energy Conversion and Management* 47 (2006) 3368–82.
- Karami N., Rahimi M., Heat transfer enhancement in a hybrid microchannel-photovoltaic cell using Boehmite nanofluid, *International Communications in Heat and Mass Transfer* 55 (2014) 45–52.
- Karami N., and Rahimi M., Heat transfer enhancement in a PV module using Boehmite nanofluid, *Energy Convers Manage* 86 (2014) 275–285.
- Khanjari Y., Pourfayaz F., Kasaeian A.B., Numerical investigation on using of nanofluid in a water-cooled photovoltaic thermal system, *Energy Convers Manage* 122 (2016) 263–78.
- Ji J., Lu X., Xu Z., Effect of ultrasonic on adsorption of Geniposide on polymeric resin, *Ultrasonic Sonochemistry* 13 (2006) 463–470.
- Liao B., Sun W.Y., Guo N., Ding S.L., Su S. J., Equilibriums and kinetics studies for adsorption of Ni (II) ion on chitosan and its triethylenetetramine derivative, *Colloids and Surfaces A: Physicochemical and Engineering Aspects* 501 (2016) 32–41.
- Malamis S., and Katsou E., A review on zinc and nickel adsorption on natural and modified zeolite, bentonite and vermiculite: Examination of process parameters, kinetics and isotherms, *Journal of Hazardous Materials* 252 (2013) 428–461.
- Menkah E.S., Dzade N.Y., Tia R., Adei E., Leeuw N.H., Hydrazine adsorption on perfect and defective fcc nickel (100), (110) and (111) surfaces: A dispersion corrected DFT-D2 study, *Applied Surface Science* 480 (2019) 1014–1024.
- Mousavi S.A., Almasi A., Navazeshkha F., Falahi F., Biosorption of lead from aqueous solutions by algae biomass: optimization and modeling, *Desalination and Water Treatment* 148 (2019) 229–237.
- Nayeri D., Mousavi S.A., Mehrabi A., Oxytetracycline removal from aqueous solutions using activated carbon prepared from corn stalks, *Journal of Applied Research in Water and Wastewater* 6 (2019) 67–72.
- Parvizian F., Rahimi M., Azimi N., Macro- and micromixing studies on a high frequency continuous tubular sono-container, *Chemical Engineering Processing* 57–58 (2012) 8–15.
- Radwan A., Ahmed M., Ookawara S., Performance enhancement of concentrated photovoltaic systems using a microchannel heat sink with nanofluids, *Energy Convers Manage* 119 (2016) 289–303.
- Rahimi M., Azimi N., Parvizian F., Using microparticles to enhance micromixing in a high frequency continuous flow sono-container, *Chemical Engineering Processing* 70 (2013) 250–258.
- Sayadi M.H., and Rezaei M.R., Impact of land use on the distribution of toxic metals in surface soils in Birjand city, *Proceedings of the International Academy of Ecology and Environmental Sciences* 4 (2014) 18–29.
- Siahkamari L., Rahimi M., Azimi N., Banibayat M., Experimental investigation on using a novel phase change material (PCM) in micro structure photovoltaic cooling system, *International Communications in Heat and Mass Transfer* 100 (2019) 60–66.
- Suresh A.K., Khurana S., Nandan G., Dwivedi G., Kumar S., Role on nanofluids in cooling solar photovoltaic cell to enhance overall efficiency, *Materials Today: Proceedings* 5 (2018) 20614–20620.
- Wang J., Xu L., Cheng C., Meng Y., Li A., Preparation of new chelating fiber with waste PET as adsorbent for fast removal of Cu^{2+} and Ni^{2+} from water: kinetic and equilibrium adsorption studies, *Chemical Engineering Journal* 193 (2012) 31–38.